BROOKHAVEN
NATIONAL LABORATORY

BNL-81256-2008-CP

Internal electric-field-lines distribution in CdZnTe detectors measured using X-ray mapping

A. E. Bolotnikov, G. S. Camarda, Y. Cui, A. Hossain, G. Yang, H. W. Yao, and R. B. James

Brookhaven National Laboratory, Upton, NY 11973

Nonproliferation and National Security Department
Detector Development and Testing Division

Brookhaven National Laboratory
P.O. Box 5000
Upton, NY 11973-5000
www.bnl.gov

DISCLAIMER

Internal electric-field-lines distribution in CdZnTe detectors measured using X-ray mapping

A. E. Bolotnikov, G. S. Camarda, Y. Cui, A. Hossain, G. Yang, H. W. Yao, and R. B. James

Brookhaven National Laboratory, Upton, NY 11973

Abstract

The ideal operation of CdZnTe devices entails having a uniformly distributed internal electric field. Such uniformity especially is critical for thick long-drift-length detectors, such as large-volume CPG and 3-D multi-pixel devices. Using a high-spatial resolution X-ray mapping technique, we investigated the distribution of the electric field in real devices. Our measurements demonstrate that in thin detectors, <5 mm, the electric field-lines tend to bend away from the side surfaces (i.e., a focusing effect). In thick detectors, >1 cm, with a large aspect ratio (thickness-to-width ratio), we observed two effects: the electric field lines bending away from or towards the side surfaces, which we called, respectively, the focusing field-line distribution and the defocusing field-line distribution. In addition to these large-scale variations, the field-line distributions were locally perturbed by the presence of extended defects and residual strains existing inside the crystals. We present our data clearly demonstrating the non-uniformity of the internal electric field.

Keywords: CdZnTe, gamma ray detectors, internal electric fields, perturbations

1. Introduction

Recently, we employed a highly collimated x-ray beam [1] to study spatial variations of the responses of CdZnTe (CZT) detectors with micron-scale resolution. The x-ray mapping system we developed for such measurements allowed us to investigate the effects of different types of microscopic defects on their performance (see the most recent publication in Ref. [2]). The system also gave us the opportunity to map the electric-field line distribution in CZT devices that we report in this paper.

The ability to maintain a desired electric field inside a CZT device is important for assuring its expected performance and functionalities. If the actual distribution of the field lines differs from the anticipated one based on the electrodes' configuration, then the charges generated by incident particles might be driven towards wrong electrodes, or become trapped in "dead" regions, e.g., near the side surfaces.

We can represent a typical CZT detector as a rectangular crystal block with contacts deposited on two opposite facets. The cathode usually is a monolithic contact that covers the entire area of the facet, while the anode may have one of the patterns that identify a particular type of device: pixel, coplanar grid, or strip. A constant lateral electric field is expected to ensure uniform efficiency in charge collection over the entire device's area down to the very edges. However, when a CZT detector (considered as metal-semiconductor-metal structure with two back-to-back Schottky barriers) is biased, a space charge is formed between the anode and cathode due to the charging/ionization of deep levels, which may create a non-uniform distribution. This modifies the electric-field distribution on a large scale, and may introduce significant local variations. Because of the space charge, the electric field is expected to be changing in the z-direction, as in any other depleted semiconductor.

There are limited experimental data on this subject [3]. The Pockels electro-optic effect (PE) was employed to investigate the distribution of the internal electric field within CZT radiation detectors [4-9]. Utilizing the slight birefringent optical property of a CZT crystal under bias, the Pockels effect showed that most such distributions in CZT detectors were non-uniform, and were related to crystal defects and grain boundaries [5]. Based on the PE data, an energy band model was proposed to describe the internal electric-field distributions in CZT detectors [6]. However, many more investigations are needed to understand the internal E-field distributions in relation to the CZT detector's performance, its crystal defects and fabrication procedures. Several groups [5,9] reported that the electric-field strength in CZT detectors is highest near the cathode and decreases towards the anode side, consistent with the accumulation of the positive ions. In contrast, CdTe detectors apparently exhibit an opposite behavior: electric-field strength

increases towards the cathode [10]. The formation of the positive space charge in CZT detectors was found to be consistent with the analysis of *I-V* curves measured for 2-mm thin planar detectors with a small geometrical-aspect ratio (thickness-to-width ratio) [11]. By fitting the *I-V* curves, the concentration of the positive ions was estimated as ~10^{10} cm^{-3}, while the concentration of the free carriers in high-resistivity CZT material is only ~10^5 cm^{-3}. As an example, at such space-charge densities, the reduction of the electric field is expected to be ~15% in a 2-mm thick detector biased at 200 V. In CZT detectors with large aspect ratios, >1, it is very likely that the variations of the electric field may not be described by a simple linear function because of the possibility of non-uniform accumulation of space charge.

The electric-field strength also can vary laterally, especially inside the devices with large aspect ratios. The conditions near the edges can differ from those in central regions of the device, causing poor charge-collection near the device's edges, called the edge effect. For peripheral events whose fractions increase as the square of the device's width, the charge-collection efficiency may be impaired because of the proximity of the side surfaces where the drift velocity is smaller than in the bulk, and the concentration of traps higher. To avoid this effect, the vector of the electric field near the side surfaces should point away from them. In other words, on a large scale, the electric field should be slightly focusing in the direction towards the anode to provide high collection efficiency near the side surfaces. Theoretically, such conditions should naturally exist inside CZT crystals with positive space charge [12]. Indeed, the electric-field distribution is determined by the boundary conditions i.e., the electrostatic potential distribution on the device's side surfaces, which, in turn, are determined by the surface conductivity. If the surface potential decreases between the cathode and the anode faster than the potential along the device's axis, a defocusing field is generated inside the device thereby diminishing the detector's performance. In the opposite case, a focusing drift-field will form inside the device that steers the electrons toward the anode. Because of the high surface conductivity, the surface potential is almost independent of the bulk and changes linearly between the cathode and anode levels. At the same time, the bulk potential decreases as a sub-linear function due to the presence of the positive space-charge. Thus, theoretically, these two effects inevitably should produce a focusing field that is more favorable for the CZT detectors. However, in practice, the distribution of the electric field is not always as predicted, based on the above considerations.

Using a highly collimated x-ray beam, available at BNL's NSLS, we routinely characterize the responses of CZT devices of different configurations. Although the main goal of these measurements is to study the influence of the crystal defects on charge-transport properties, we can also map the distribution of the electric-field lines and their local variations. In this paper, we present the results from such mapping that we carried on two CZT pixel detectors, one thin and one thick. Our goal is to emphasize the surprisingly strong discrepancies between the expected and actual field-line distributions in high-quality commercial CZT detectors.

2. Experimental

The details of the high-spatial resolution x-ray mapping system used in these studies are described elsewhere [2]. Briefly, we employed a monochromatic (10-30) keV x-ray beam with a spot size of less than 25x25 μm^2 to generate free carriers and study charge transport in CZT samples. For each position of the beam, a pulse-height spectrum was collected and evaluated to locate a central gravity of the peak, which is proportional to the fraction of the collected charge originally generated near the cathode. These values, plotted as a 2D map, represent the device's response. This system allows us to carry out a variety of measurements, including mapping the distributions of the electric field lines in different types of CZT detectors. Here, we discuss the line maps obtained from two commercial 1x1x1 cm^3 4x4 pixel detectors (D1 and D2) that are representative of two limiting cases of the CZT device's behaviors. The pixel contacts were interconnected together in a way to form two electrodes somewhat resembling a chessboard (Fig. 1). In our discussion, we will call them black and white contacts. The charge signals, generated by the x-ray beam pointed in a particular location of the cathode surface, were read out using only one electrode while the second one was grounded. In the ideal case of a uniform electric-field distribution inside a crystal, a raster scan over the entire area of the device would generate a response map with a pattern identical to those of the electrode used to read the signals. A distorted pattern measured from a real device would signify the deviation of the actual electric-field distribution from uniformity. A standard eV Products preamplifier was used to read the signals, which were further shaped and amplified with a standard research amplifier. During the measurements, we applied a negative 1000 V bias to the detectors' cathodes.

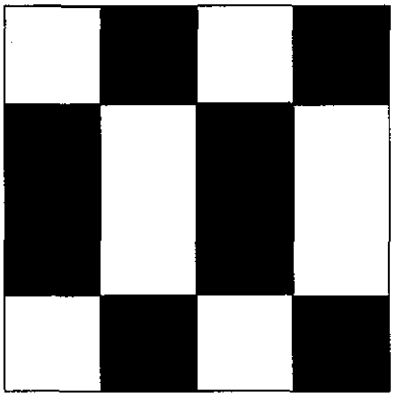

Fig. 1. Electrode patterns (black and white) formed by interconnecting individual pixel contacts.

3. Results and discussion

Fig. 2 (a-d) shows the response maps measured for the detector D1: (a) The black contacts are grounded, (b) the same as (a) but after applying a filter to highlight the pixels' boundaries, (c) all pixels are connected to form a monolithic contact used to read signals, and, (d) the same as (c) but after filtering to highlight the local variations in the detector's response caused by Te inclusions and twin boundaries. The dark colors represent the areas where weak signals were detected. Note, that when the grounded electrode collects electrons from the electron cloud, small signals still are induced by the electrons trapped in the bulk. The light colors represent strong signals induced by the electrons collected by the electrode used to read the signals (except for small regions corresponding to the crystal's defects). To see more clearly the deviations of the actual electric-field distribution from uniformity, we have overlaid a grid indicating the geometrical boundaries of the actual pixels. We note that crystal defects, such as inclusions and twin boundaries, also appear as dark areas. For example, a twin boundary is located in the crystal's upper left corner. The electric field, distorted by this boundary, steers electrons to the side surfaces where they become trapped. The individual inclusions are dispersed everywhere within the crystal. Also, there is a network of inclusions (or dislocations) near the upper edge of the crystal.

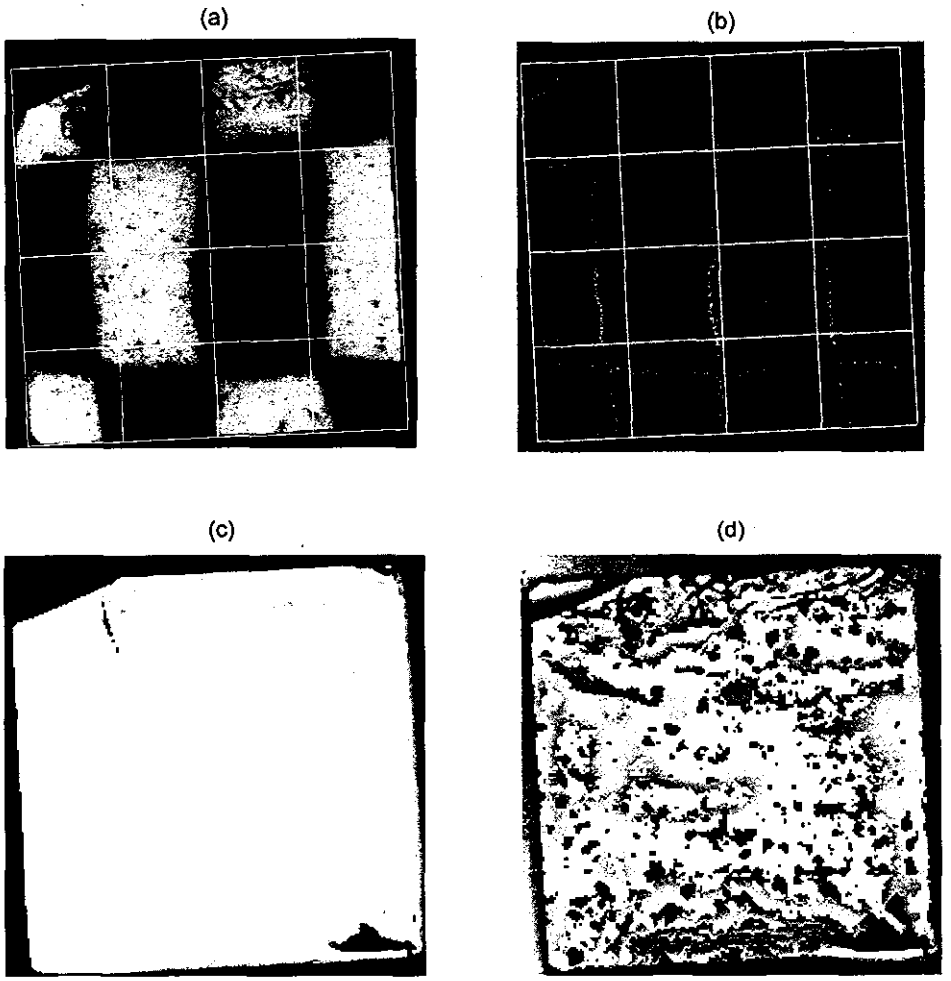

Fig. 2. Response maps acquired for detector D1: (a) Black pixels are grounded, (b) same as (a) but after applying a filter to highlight the pixels' boundaries, (c) all pixels are connected to form a single contact used to read signals, and, (d) same as (c) but after filtering to highlight the areas with defects (inclusions and twin boundaries). The grids represent the geometrical locations of the pixel contacts. The step size is 50 μm, and the total scan area is ~12x12 mm^2.

Comparing the apparent footprints of pixels f and actual pixel clearly reveals that the electric field inside the thick CZT crystals is far from uniform. Fig. 2(a) shows that the apparent footprints of the pixels adjacent to the crystal's edges are notably smaller than their actual sizes. On the other hand, the apparent footprints of four central pixels stretch beyond their actual boundaries, while their internal boundaries are correctly located in the middle of the detector. Such patterns indicate that electron clouds originating at the cathode drift some distances laterally towards the center of the device before arriving at the anode. In other words, detector D1 has a focusing electric field, which is schematically shown in Fig. 3(a). (The field in Fig. 3 (a,b) represents an exact solution of the Dirichlet problem in a 2D case.) The apparent locations of the contacts are shown on the cathode side are obtained by the backward projecting of the actual contacts along the electric-field lines. Such an electric field is expected if the electrostatic potential in the bulk of the crystal changes faster (from the cathode and anode) than the potential along its side surfaces. This can occur when there is a positive space-charge in the sample. Because of the focusing field, the detector D1 shows good response from the entire area of the crystal down to its very edges, as illustrated in Fig. 2(c).

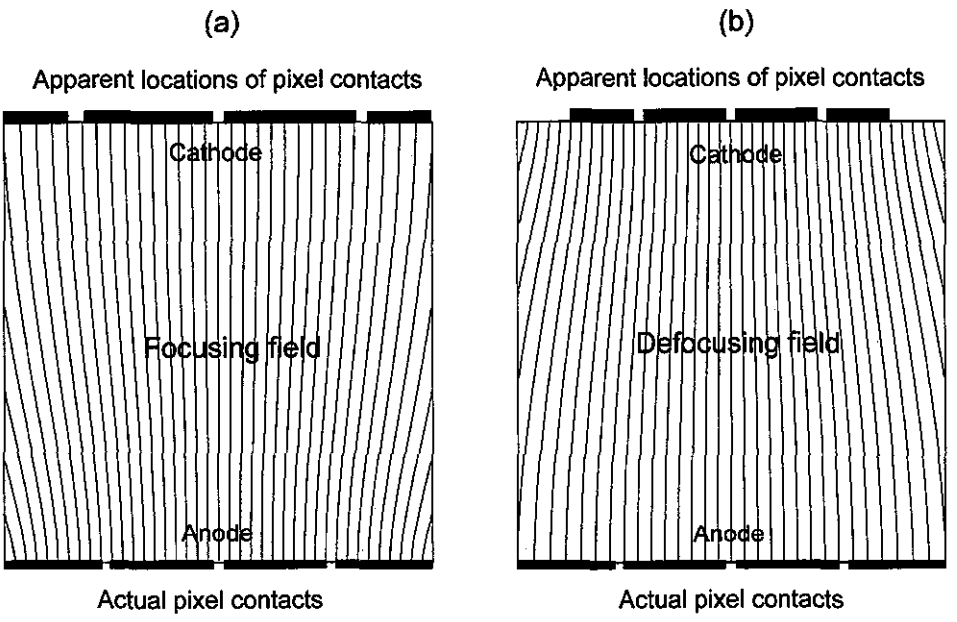

Fig. 3. Electric-field-line distributions modeled for a CZT sample, 1-mm thick by 1-mm wide with an infinite third direction, illustrating the focusing (a), and defocusing (b) fields in the detectors D1 and D2, respectively.

Fig. 4 are response maps similar to those shown in Fig. 2 but measured for the detector D2: (a) Black contacts are grounded, (b) white contacts are grounded, (c) all pixels are connected together as a single contact to read signals, and, (d) same as (c) but after filtering to highlight local variations in the detector's response. The detector D2 represents a defocusing electric field, for which the field lines are bent towards the side surfaces of the crystal (Fig. 3(b)). The apparent pixels near the edges, in Figs. 4(a) and (b), are significantly smaller than their actual sizes. In fact, the field lines are so strongly bent that some of the edge pixels do not collect any charges, while some central pixels have reduced footprints. This is because all the electrons generated at the cathode above these pixels are driven to the side surface, where they become trapped. In other words, this detector D2 suffers from the edge effect caused by the defocusing electric field distribution inside the crystal. Following the same considerations we applied to the previous case, one can conclude that the detector D2 has negative space charge.

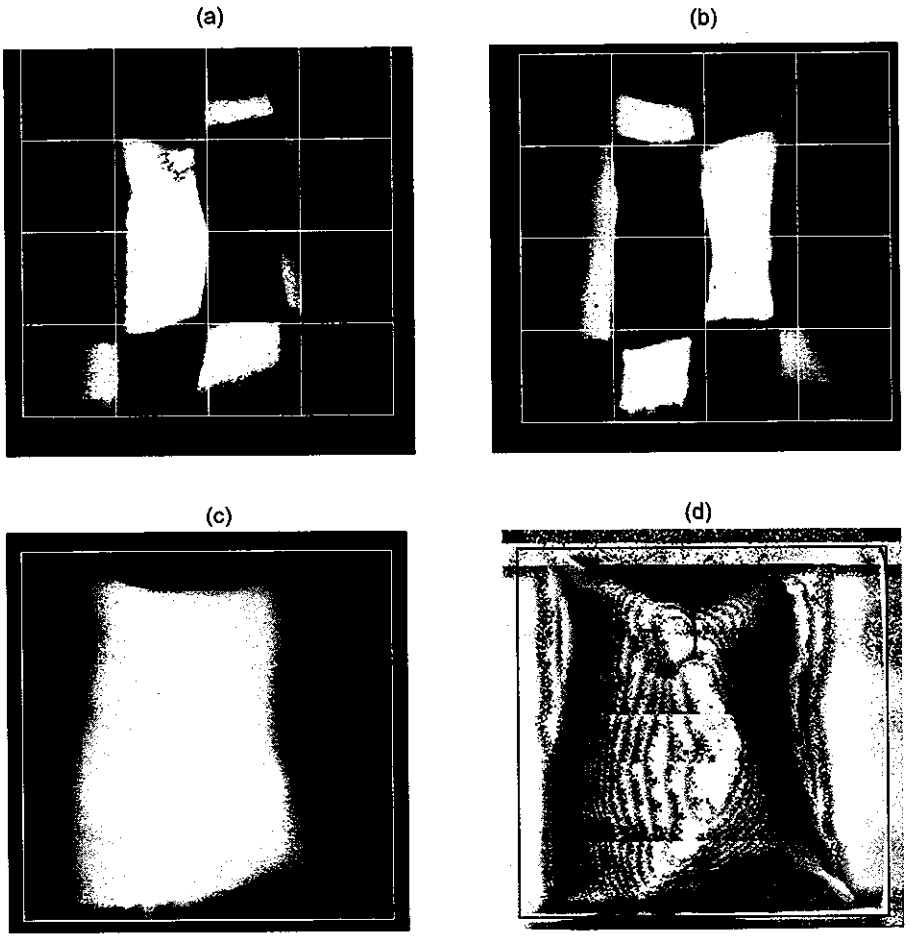

Fig. 4. Response maps measured for the detector D2: (a) Black pixels are grounded, (b) white pixels are grounded, (c) all pixels are connected together and used to read signals, and, (d) same as (c) but after filtering to highlight the extended defects. The grids represent geometrical locations of the contacts on the anode side. Spatial resolution is 50 μm, and the total scan area ~12x12 mm^2.

Clearly, a defocusing electric field causes an undesirable charge loss near the device's edges in thick CZT detectors. As discussed in the introduction, to avoid this edge effect the electrostatic potential on the side surfaces should change slower than that in the balk. This can be achieved by slightly extending (by 2-3 mm) the cathode electrode on the side surfaces, as in the CAPture device [13,14]. To illustrate the idea, Fig. 5 compares the distributions of field lines calculated in a 2D approximation (for simplicity) for a detector, 1-cm thick by 1-cm wide and an infinite third direction, with two cathode geometries: (a) Conventional, and, (b) with an extended cathode. In both cases, we assumed that the potential on the side surfaces changes linearly from the cathode voltage down to zero, and no space charge accumulates in the bulk.

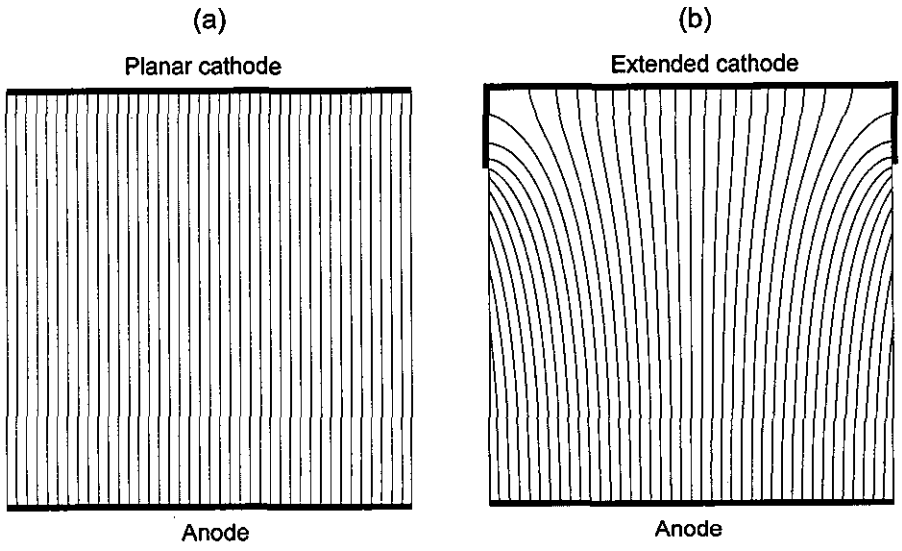

Fig. 5. Comparison between the distribution of field lines calculated in a 2D approximation for a detector, 1-cm thick by 1-cm wide with an infinite third direction, with two cathode geometries: (a) Conventional, and, (b) with the extended cathode. A linearly changing potential on the side surfaces and no space-charge accumulation were assumed. The cathode extends 2 mm along the side surfaces.

So far, we discussed two possible cases of the global distribution of the electric-field lines inside CZT crystals, illustrated in Figs. 2 and 4. These same figures also indicate local variations of the electric field that can be seen in the response maps as wavy boundaries and chipped pixels. We attribute some of these variations to the inclusions and twins that are clearly apparent in the filtered response map (d) of detector D1. However, there are no defects seen for the detector D2, even though the maps were generated with higher resolution, in 25 μm steps. Also, the typical size of the local field variations is notably larger than the average size of the inclusions. From these findings, we conclude that certain material (bulk and surface) defects do not trap charge but affect the local electric field. The most reasonable candidates for such defects could be strains in the crystals, and associated with them, dislocations networks that locally accumulate the space charge.

4. Conclusions

A uniform electric field is especially critical for thick long-drift-length detectors, such as large-volume CPG and 3-D multi-pixel devices. It should be considered as a real factor degrading performance of CZT detectors. Using a high-spatial resolution X-ray mapping technique, we investigated the distribution of the electric field in real devices. Our previous measurements demonstrate that in thin, <5 mm, CZT detectors, the electric field lines have a tendency to bend away from the side surfaces (the focusing effect). However, in thick detectors, >10 mm, the distribution of field lines depends on the polarity and distribution of the space charge accumulated inside the biased device, and on the electronic properties of the side surfaces that define the boundary conditions for the electrostatic potential. If the potential on the side surface decreases (in absolute values) more slowly than in the bulk, a focusing electric field is expected. In the opposite case, the field will be a defocusing one that engenders a loss in collection charge near the edges.

We also found that the electric field was significantly perturbed by the presence of extended defects and the residual strains existing inside the crystals.

ACKNOWLEDGEMENTS

This work was supported by U.S. Department of Energy, Office of Nonproliferation Research and Development, NA-22. The manuscript has been authored by Brookhaven Science Associates, LLC under

Contract No. DE-AC02-98CH1-886 with the U.S. Department of Energy. The United States Government retains, and the publisher, by accepting the article for publication, acknowledges, a world-wide license to publish or reproduce the published form of this manuscript, or allow others to do so, for the United States Government purposes.

REFERENCES

[1] G. A. Carini, A. E. Bolotnikov, G. S. Camarda, G. W. Wright, L. Li, and R. B. James, "Effect of Te precipitates on the performance of CdZnTe detectors", Appl. Phys. Lett. 88, p. 143515, 2006.

[2] G. S. Camarda, A. E. Bolotnikov, Y. Cui, A. Hossain, S. A. Awadalla, J. Mackenzie, H. Chen, and R. B. James, "Polarization Studies of CdZnTe Detectors using Synchrotron X-ray Radiation", submited to IEEE Trans. Nucl. Sci., 2008.

[3] James L. Matteson, Wayne Coburn, Fred Duttweiller, William A. Heindl, George L. Huszar, Philippe C. Leblanc, Michael R. Pelling, Laurence E. Peterson, Richard E. Rothschild, and Robert T. Skelton, "CdZnTe arrays for astrophysics applications", Hard X-Ray and Gamma-Ray Detector Physics, Optics, and Applications, edited by Richard B. Hoover, F. P. Doty, Proceedings of SPIE Vol. 3115, pp. 160-175, 1997.

[4] R. Guenther, "Modern Optics", John Wiley & Sons, Inc. pp 569-590, 1990.

[5] H. W. Yao, R. B. James, E. Y. Lee, R. W. Olsen, H. Hermon, and R. J. Anderson, "Optical Studies of the Internal Electric Field Distributions, Crystal Defects and Detector Performance of CdZnTe Radiation Detectors", SPIE Proceedings, 3446, pp. 169-178, 1998.

[6] H. W. Yao, R. J. Anderson, and R. B. James, "Optical Characterization of the Internal Electric Field Distribution under Bias of CdZnTe Radiation Detectors", SPIE Proceedings, 3115, pp 62-68, 1997.

[7] H. W. Yao R. J. Anderson, R. B. James, and R. W. Olsen, Mater. "Optical Studies of the Internal Electric Field Distributions of CdZnTe Detectors Under Bias Conditions", Res. Soc. Symp. Proc. 487, pp 51-57, 1998.

[8] H. W. Yao, R. B. James, and E. C. Erickson, "Optical Engineering and Characterization of the Internal Electric Field of CdZnTe Radiation Detectors", SPIE Proceedings 3768, pp. 330-338, 1999.

[9] M. A. Hossain, E. J. Morton, and M. E. Özsan, "Photo-Electronic Investigation of CdZnTe Spectral Detectors", IEEE Trans. Nucl. Sci., V. 49, No. 4, pp. 1960-1964, 2002.

[10] A. Cola, I. Farella, A. M. Mancini, and A. Donati, "Electric Field Properties of CdTe Nuclear Detectors", IEEE Trans. Nucl. Sci., V. 54, pp. 868-872, 2007.

[11] A. E. Bolotnikov, S. E. Boggs, C. M. Hubert Chen, W. R. Cook, F. A. Harrison, and S. M. Schindler, "Properties of Pt Schottky Type Contacts On High-Resistivity CdZnTe Detectors", *Nucl. Instr. Meth.*, A482, pp. 395-407, 2002.

[12] A. E. Bolotnikov, N. M. Abdul-Jabbar, S. Babalola, G. S. Camarda, Y. Cui, A. Hossain, E. Jackson, H. Jackson, J. R. James, A. L. Luryi, and R. B. James, "Optimization of virtual Frisch-grid CdZnTe detector designs for imaging and spectroscopy of gamma rays", Proceedings of SPIE Conference on Hard X-Ray and Gamma-Ray Detector Physics IX, Vol. 6706, edited by R. B. James, A. Burger, L. A. Franks, San Diego, CA, pp. 670603-1-13.

[13] K. Parnham, C. Szeles, K. G. Lynn, R. Tjossem, "Performance Improvement of CdZnTe Detectors Using Modified Two-Terminal Electrode Geometry," in Hard X-ray, Gamma-Ray and Neutron Detector Physics, Proceedings of SPIE, Vol. 3786, pp. 49-54, 1999.

[14] C. Szeles, D. Bale, J. Grosholz, Jr., G. L. Smith, M. Blostein, and J. Eger, "Fabrication of High Performance CdZnTe Quasi-Hemispherical Gamma-ray CAPture™ Plus Detectors", in Hard X-Ray and Gamma-Ray Detector Physics VIII, edited by Larry A. Franks, Arnold Burger, and Ralph B. James, Proceedings of SPIE Vol. 6319, pp. 63190B-1 - 63190B-1, 2006.